Effect of CaO content in raw material on the mineral composition of ferric-rich sulfoaluminate clinker

Yao, Xingliang; Yang, Shizhao; Dong, Hua; Wu, Shuang; Liang, Xuhui; Wang, Wenlong

DOI
10.1016/j.conbuildmat.2020.120431

Publication date
2020

Document Version
Accepted author manuscript

Published in
Construction and Building Materials

Citation (APA)
Yao, X., Yang, S., Dong, H., Wu, S., Liang, X., & Wang, W. (2020). Effect of CaO content in raw material on the mineral composition of ferric-rich sulfoaluminate clinker. *Construction and Building Materials*, *263*, Article 120431. https://doi.org/10.1016/j.conbuildmat.2020.120431

Effect of CaO content in raw material on the mineral composition of ferric-rich sulfoaluminate clinker

Xingliang Yao [a, b], Shizhao Yang [a], Hua Dong [b], Shuang Wu [a], Xuhui Liang [b], Wenlong Wang [a,*]

[a] National Engineering Laboratory for Reducing Emissions from Coal Combustion, Engineering Research Center of Environmental Thermal Technology of Ministry of Education, Shandong Key Laboratory of Energy Carbon Reduction and Resource Utilization, School of Energy and Power Engineering, Shandong University, Jinan, Shandong, 250061, China

[b] Microlab, Faculty of Civil Engineering and Geosciences, Delft University of Technology, 2628 CN Delft, The Netherlands

Abstract

Ferric-rich calcium sulfoaluminate (FR-CSA) cement is an eco-friendly cement. Fe_2O_3 exists in different minerals of FR-CSA clinker, e.g., $Ca_4Al_2Fe_2O_{10}$ (C_4AF), $Ca_2Fe_2O_5$ (C_2F), and $Ca_4Al_{6-2x}Fe_{2x}SO_{16}$ ($C_4A_{3-x}F_x\bar{S}$). The mineral composition depends on the chemical composition of the raw materials and significantly determines the reactivity of FR-CSA cement. To optimize the phase composition of the FR-CSA clinker, chemical reagent raw mixtures with different amounts of CaO were used to prepare the FR-CSA clinker. X-ray diffraction (XRD) analysis, Rietveld quantitative phase analysis (RQPA), Fourier Transform Infrared spectroscopy (FT-IR), and scanning electron microscopy/energy-dispersive spectroscopy (SEM/EDS) were used to identify the mineralogical conditions of the FR-CSA clinker. The results indicated that the amounts of CaO in raw materials greatly affected the iron-bearing phase formation in the FR-CSA clinker. With decreasing CaO content involved in calcination reaction, the amounts of Fe_2O_3 incorporated in $C_4A_{3-x}F_x\bar{S}$ increased up to 17.72 wt.% (where x = 0.36). The findings make it possible to optimize the mineral composition of the FR-CSA clinker by changing the CaO content in raw materials. Furthermore, low CaO content in the raw material is beneficial to the formation of $C_4A_{3-x}F_x\bar{S}$, which enables the use of solid wastes containing low calcium for producing FR-CSA cement.

Keywords: Ferric-rich sulfoaluminate cement, CaO, Optimization, Phase composition, Iron-bearing phase

1. Introduction

Calcium sulfoaluminate (CSA) cement is a new type of cement first developed in China 40 years ago. It exhibits some great performances, such as high early strength, rapid setting, and shrinkage-compensating, et al. for certain applications [1-3]. The major phases of CSA clinker are ye'elimite ($Ca_4Al_6SO_{16}$, $C_4A_3\bar{S}$), belite (Ca_2SiO_4, C_2S), and the minor phases are anhydrite ($CaSO_4$, $C\bar{S}$), brownmillerite ($Ca_4Al_2Fe_2O_{10}$, C_4AF), and $Ca_2Fe_2O_5$ (C_2F), et al[4, 5]. $C_4A_3\bar{S}$ in CSA contains smaller amount of CaO than the alite (Ca_3SiO_5, C_3S) in Portland cement (PC). Therefore, the production of CSA clinker requires lower amount of limestone consumption compared with Portland cement (PC) production, and reduces the CO_2 emission [6]. Meanwhile, the preparation temperature of CSA clinker ranges from 1200-1300 ℃, which is 200 ℃ lower than the calcination temperature of Portland cement clinker, reducing energy consumption during the calcination process[7, 8]. Besides, the CSA clinkers are easier to grind due to their high porosity, which further reduces energy consumption during the grinding process. Therefore, the characters of energy-saving, low CO_2 emission, and good mechanical performance, make CSA cement as an ideal alternative to PC in certain applications.

However, the utilization of CSA cement is still limited. The main obstacle to the application of CSA cement on a massive scale is its high cost of raw materials, which requires expensive natural bauxite. Therefore, the consumption of bauxite, which contains high amount of Al_2O_3, should be

minimized. Fe_2O_3 is usually used as an alternative component to Al_2O_3 during the production process of CSA clinker, resulting in the FR-CSA cement. Note that the required amount of Fe_2O_3 in the FR-CSA clinker ranges from 5 to 13 wt.%, while only 1 to 3 wt.% of Fe_2O_3 exist in the CSA clinker [9]. In addition to C_2F and C_4AF, the Fe_2O_3 can also be incorporated in $C_4A_3\bar{S}$ to form $C_4A_{3-x}F_x\bar{S}$ in the FR-CSA clinker, where the value of x represents the amount of Fe_2O_3 incorporated in $C_4A_3\bar{S}$ [10, 11]. Similar to the reaction of $C_4A_3\bar{S}$ with water, $C_4A_{3-x}F_x\bar{S}$ can react with water and form ettringite, which is conducive to the development of compressive strength [9]. Thus, Fe_2O_3 can be used as a partial replacement of Al_2O_3 to reduce the consumption of aluminum source. With the reduced requirement of the consumption of aluminum source, some aluminum-bearing solid wastes or low-grade Al_2O_3 minerals can be used, and the cost of FR-CSA cement can be reduced.

During the calcination process of the FR-CSA clinker, the distributions of Fe_2O_3 in iron-bearing phases are affected by the chemical composition of the raw material. And the iron-bearing phase composition influences the mechanical properties of the FR-CSA cement [12, 13]. To optimize the iron-bearing phase composition of FR-CSA clinker, it is important to know the effect of raw material composition on the iron-bearing phase formation in the FR-CSA clinker. Many researchers have investigated the effect of raw material on the phase composition of the FR-CSA clinker. Y. Huang et al. concluded that the addition of Fe_2O_3 could promote higher **Fe_2O_3** incorporation into CSA clinker, forming $C_4A_{2.7}F_{0.3}\bar{S}$ [14]. Dun Chen et al. studied the effect of Fe_2O_3 content on the incorporation level of Fe_2O_3 into $C_4A_{3-x}F_x\bar{S}$ and concluded that 22.31 wt.% Fe_2O_3 reached maximum incorporation content into $C_4A_{3-x}F_x\bar{S}$[10]. Idrissi M. et al. identified the mineralogical conditions of iron inclusion during the formation of $C_4A_3\bar{S}$ made from different raw materials. The maximum fraction of Fe_2O_3 in the $C_4A_3\bar{S}$ was 21.5 wt.%[15]. Bruno Touzo et al. studied the phase equilibria in the $CaO–Al_2O_3–Fe_2O_3–SO_3$ system at 1325 ℃ and got that the value of x increased to a plateau of 0.34[16]. All the aforementioned researches were focused on the effect of $Fe_2O_3/(Fe_2O_3+Al_2O_3)$ ratio in $CaO–Al_2O_3–Fe_2O_3–SO_3$ system. However, CaO is a primary content in the FR-CSA clinker. During the calcination of FR-CSA clinker, CaO almost participates in all the phase formation reactions and distributes in all minerals according to Eqs. 1– 8[17]. Thus, CaO content is a critical parameter for the phase composition in FR-CSA clinker.

Bruno Touzo et al. also put forward that $Fe_2O_3/(Fe_2O_3+Al_2O_3)$ was not the only parameter influencing the value of x. The CaO content and the content of other elements would shift the equilibrium of the reactions during calcination. C. Ren et al. and Y. Shen et al. prepared the CSA clinker from solid wastes and demonstrated that the CaO or $CaSO_4$ content affected the formation of C_2AS and $C_4A_3\bar{S}$ in CSA clinker[18, 19]. However, all the researches were about the effect of CaO content on phase formation or $C_4A_3\bar{S}$ in CSA clinker. Investigation on the effect of CaO content on the formation of iron-bearing phases in FR-CSA clinker is still limited. To optimize the iron-bearing phase composition of the FR-CSA clinker, it is necessary to investigate the effect of CaO content on the iron-bearing phase formation in FR-CSA clinker.

$$Ca(OH)_2 \xrightarrow{500\ ^\circ C} CaO+H_2O \quad \text{Eq. 1}$$

$$CaCO_3 \xrightarrow{800\text{-}850\ ^\circ C} CO_2+CaO \quad \text{Eq. 2}$$

$$2CaO+Al_2O_3+SiO_2 \xrightarrow{900\text{-}950\ ^\circ C} C_2AS \quad \text{Eq. 3}$$

$$3CaO+3Al_2O_3+CaSO_4 \xrightarrow{950\text{-}1000\ ^\circ C} C_4A_3\bar{S} \quad \text{Eq. 4}$$

$$3CaO+3C_2AS+CaSO_4 \xrightarrow{1050\text{-}1150\ ^\circ C} C_4A_3\bar{S}+3C_2S \quad \text{Eq. 5}$$

$$2CaSO_4 \xrightarrow{1170\ ^\circ C} SO_2+CaO+O_2 \quad \text{Eq. 6}$$

$$2CaO+Fe_2O_3 \xrightarrow{1000\text{-}1100\ ^\circ C} C_2F \quad \text{Eq. 7}$$

$$2CaO+C_2F+Al_2O_3 \xrightarrow{1150\text{-}1200\ ^\circ C} C_4AF \quad \text{Eq. 8}$$

The aim of this work is to investigate the feasibility of optimizing the phase composition of FR-CSA clinker by changing the CaO content in raw materials. In our research, the FR-CSA clinkers were prepared from chemical reagents, in which different amount of $Ca(OH)_2$ and $CaSO_4$ were added to change the CaO content, respectively. X-ray diffraction (XRD) analysis, Rietveld quantitative phase analyses (RQPA), and Fourier Transform Infrared spectroscopy (FT-IR) were used to identify and quantify the phase composition, respectively. Scanning electron microscopy/energy-dispersive spectroscopy (SEM/EDS) was used to detect the distribution of Fe_2O_3 in iron-bearing phases. Along with the variation of iron-bearing phase compositions, the incorporated content of Fe_2O_3 in $C_4A_{3-x}F_x\bar{S}$ was calculated. The effective utilizations of Fe_2O_3 and Al_2O_3 in the FR-CSA clinker were also calculated according to the distribution of Fe_2O_3 and Al_2O_3 in different phases. Finally, the clinkers with different C_4AF designed and with different calcination process were also got to certify the effect of CaO content in raw materials.

2. Experiment

2.1 Preparation of FR-CSA clinker

2.1.1 Raw materials

The chemical pure reagents ($Ca(OH)_2$, Al_2O_3, $CaSO_4$, Fe_2O_3, and SiO_2), which were supplied by Sinopharm Group Chemical Reagent Co., Ltd., Shanghai, China, were used as raw materials to prepare the FR-CSA clinker. Among them, $Ca(OH)_2$ was used as the source of CaO. $CaSO_4$ was not only used as the source of CaO but also was the source of SO_3 during the calcination process of the FR-CSA clinker.

The FR-CSA clinker was synthesized from chemical reagent raw materials based on stoichiometric amount. The ratios of raw materials were calculated according to the Bogue method, which was adapted for CSA clinker by assuming phase assemblage of C_2S, $C_4A_3\bar{S}$, C_4AF, and $CaSO_4$ as given in Eqs. 9-12[20]:

$$C_4AF\%=(F\%)\times\left(\frac{M_{C_4AF}}{M_F}\right) \quad \text{Eq. 9}$$

$$C_2S\%=(S\%)\times\left(\frac{M_{C_2S}}{M_S}\right) \quad \text{Eq. 10}$$

$$C_4A_3\bar{S}\%=\left(A\%-C_4AF\%\times\frac{M_A}{M_{C_4AF}}\right)\times\frac{M_{C_4A_3\bar{S}}}{3\times M_A} \quad \text{Eq. 11}$$

$$C\bar{S}\%=\left(\bar{S}\%-C_4A_3\bar{S}\%\times\frac{M_{\bar{S}}}{M_{C_4A_3\bar{S}}}\right)\times\frac{M_{C\bar{S}}}{M_{\bar{S}}} \quad \text{Eq. 12}$$

The CaO content in the FR-CSA clinkers was termed as the alkalinity modulus (C_m) and defined using Eq. 13[9]. The value of *x* indicates the degree to which CaO in the raw material satisfies the reaction with SiO_2, Al_2O_3, and Fe_2O_3 to form useful minerals (i.e., $C_4A_3\bar{S}$, C_4AF, and C_2S) in the CSA

clinker. It is usually lower than 1.00 to avoid the existence of free calcium oxide (f-CaO) in the CSA clinker. The C_m is calculated as follows.

$$C_m=\frac{CaO-0.7TiO_2}{1.87SiO_2+0.73(Al_2O_3-0.64Fe_2O_3)+1.40Fe_2O_3} \quad \text{Eq. 13}$$

According to Table 1 and Eq. 9-12, five FR-CSA clinkers with different CaO content were designed and termed as $C_{0.90}$, $C_{0.95}$, $C_{1.00}$, $C_{1.05}$, and $C_{1.10}$, corresponding to the C_m values of 0.90, 0.95, 1.00, 1.05, and 1.10, respectively. The targeted phase ratio of $C_4A_3\bar{S}$: C_4AF: C_2S: $CaSO_4$ was 40 %: 20 %: 30 %: 10 % by mass. Furthermore, to verify the results from the above raw mixture, as shown in Table 2, another raw mixture that targeted phase ratio of $C_4A_3\bar{S}$: C_4AF: C_2S: $CaSO_4$ was 30 %: 30 %: 30 %: 10 % by mass was also designed and termed as $C_{0.90\text{-}1}$, $C_{0.95\text{-}1}$, $C_{1.00\text{-}1}$, $C_{1.05\text{-}1}$, and $C_{1.10\text{-}1}$.

Table 1 Chemical composition in raw mixture and targeted phase compositions for FR-CSA clinkers

	Variation	Proportions (wt.%)				
		$C_{0.90}$	$C_{0.95}$	$C_{1.00}$	$C_{1.05}$	$C_{1.10}$
FR-CSA clinker	$C_4A_3\bar{S}$	40	40	40	40	40
	C_2S	30	30	30	30	30
	C_4AF	20	20	20	20	20
	$CaSO_4$	10	10	10	10	10
	C_m	**0.90**	**0.95**	**1.00**	**1.05**	**1.10**
Raw material	**CaO**	**31.3**	**33.5**	**35.7**	**38.0**	**40.2**
	SiO_2	10.7	10.7	10.7	10.7	10.7
	$CaSO_4$	21.7	21.7	21.7	21.7	21.7
	Al_2O_3	24.9	24.9	24.9	24.9	24.9
	Fe_2O_3	6.8	6.8	6.8	6.8	6.8

In addition, CaO exists in the form of $Ca(OH)_2$ and $CaSO_4$. The decomposition temperature of $Ca(OH)_2$ is below 900 ℃, which is lower than the formation temperature of $C_4A_3\bar{S}$, C_2S, C_4AF, and C_2AS. However, the decomposition temperature of $CaSO_4$ is higher than 1170 ℃. Thus, the amount of $CaSO_4$ further affects the formation of minerals in FR-CSA clinker, which is not the same as the effect of CaO content. To explore the effect of CaO in the form of $CaSO_4$ on the phase formation of FR-CSA clinker, as shown in Table 2, another five clinkers with different $CaSO_4$ contents but same C_m, termed as S_0, S_5, S_{10}, S_{15}, and S_{20}, were designed. The extra content of $CaSO_4$ was 0, 5, 10, 15, and 20 wt.% in FR-CSA clinkers, respectively. The value of C_m was 1.00 and Al_2O_3/Fe_2O_3 ratios were same for all the clinkers.

Table 2 Targeted phase compositions of the FR-CSA clinkers

Targeted phases/Variation	Proportions (wt.%)									
	$C_{0.90\text{-}1}$	$C_{0.95\text{-}1}$	$C_{1.00\text{-}1}$	$C_{1.05\text{-}1}$	$C_{1.10\text{-}1}$	S_0	S_5	S_{10}	S_{15}	S_{20}
$C_4A_3\bar{S}$	30	30	30	30	30	50	47.5	45	42.5	40
C_2S	30	30	30	30	30	30	28.5	27	25.5	24
C_4AF	30	30	30	30	30	20	19	18	17	16
$CaSO_4$	10	10	10	10	10	**0**	**5**	**10**	**15**	**20**
C_m	**0.90**	**0.95**	**1.00**	**1.05**	**1.10**	1.00	1.00	1.00	1.00	1.00

2.1.2 Preparation process

The raw materials were dried at 105 ± 5 ℃ until constant weight. Next, raw materials with a certain ratio were ground and sieved through a 200-mesh sieve to obtain the desired raw mixture. Then the raw mixture was calcined at 1250 ℃ for 30 min, and rapidly cooled at 20 ℃ to obtain FR-CSA clinkers. Finally, it was ground and sieved through a 200-mesh sieve for the following analyses.

2.2 Characterization methods

The f-CaO content in the FR-CSA clinkers was determined by the phenyl formic acid titration method in accordance with the Chinese standard GB/T 176-2017[21].

The mineral composition of different clinkers was identified using an X-ray diffractometer (Aeris, MalvernPanalytical, Netherlands) with Cu-Ka radiation at 40 kV and 15 mA. The measurement time was 0.5 h per pattern with a scanning speed of 0.6 °/min during the 2θ range of 10–50 °for qualitative analysis. RQPA was applied to perform a quantitative phase analysis using X'Pert HighScore Plus software. The crystallographic structures of phases involved in RQPA were listed in Table 3. Except for $C_4A_{3-x}F_x\bar{S}$, which was described using a refined crystallographic structure, other minerals remained the same with the reference phases. The refinement parameters were in order as follows: emission profile, background coefficients, instrument parameters, zero error, Lorentz polarization factor, unit cell parameters and preferred orientation coefficient.

Table 3 Crystallographic structures of phases involved in the RQPA

Phase	Space Group	ICSD code	Phase	Space Group	ICSD code
$C_4A_3\bar{S}$-o	I-43m	80361	$C_4A_3\bar{S}$-c	Pcc2	9560
C_2S-be	P121/nl	79551	C_2S-al'	Pnma	81097
C_4AF	Ibm2	9197	$CaSO_4$	Bmmb	16382
C_2AS	P-421m	87144	$C_5S_2\bar{S}$	Pnma	85123
C_2F	Pnma	15059	Si	Fd-3mS	29287

The FT-IR spectra of the FR-CSA clinkers were obtained using a Nicolet iS (Thermo Fisher, USA). For the analysis of the different FR-CSA clinkers, 2 mg powder samples were obtained by grinding the clinker in 400 mg of KBr. FT-IR scans were performed at frequencies from 400 cm^{-1} to 1200 cm^{-1} with a resolution of 4 cm^{-1} at 20 ℃. The results were analyzed using OMNIC software.

SEM (JSM-IT500HR, JEOL, Japan) with the 5 kV accelerated voltage was used to scan the clinker particles after Au coating treatment. SEM and EDS-mapping pictures were got to investigate the distribution of elements in the iron-bearing mineral grains.

3. Results and discussion

3.1 Analysis of FR-CSA clinkers with different amount of CaO in raw material

3.1.1 Mineralogical characterization of different FR-CSA clinkers

Fig. 1 shows the XRD patterns of the different FR-CSA clinkers. The main phases of clinkers are $C_4A_3\bar{S}$, C_2S, $CaSO_4$, C_4AF, and C_2AS. The characteristic peak intensities of C_4AF and $CaSO_4$ increase dramatically with increasing $Ca(OH)_2$. The peaks of C_2AS are only visible in clinker $C_{0.90}$. Moreover, a slight d-spaces offset for the highest peak of $C_4A_3\bar{S}$ (the cell parameter of $C_4A_3\bar{S}$-c and $C_4A_3\bar{S}$-o are (2 1 1) and (0 2 2), respectively) are observed. The d-spaces of clinkers $C_{0.90}$, $C_{0.95}$, $C_{1.00}$, $C_{1.05}$, and $C_{1.10}$ are 3.7627, 3.7621, 3.7612, 3.7596, and 3.7587 Å, respectively. With increasing CaO content in raw material, the d-spaces decrease from 3.7627 to 3.7587 Å. It is speculated that some Fe_2O_3 is incorporated in $C_4A_3\bar{S}$ mineral to form $C_4A_{3-x}F_x\bar{S}$ in the FR-CSA clinker. The radius of Fe^{3+} (r=0.069 nm) is larger than that of Al^{3+} (r=0.053 nm)[22]. Fe^{3+} occupies the octahedral position, whereas Al^{3+}

occupies the tetrahedral position in the $C_4A_{3-x}F_x\bar{S}$. Thus, with increasing CaO content, the content of Fe_2O_3 incorporated into $C_4A_{3-x}F_x\bar{S}$ may decreases, which leads to a decrease in the volume of the unit cell structure of $C_4A_{3-x}F_x\bar{S}$ phase and a shift of the d-space of the main peak to a smaller value.

In addition, the interplanar spacing of $C_4A_{3-x}F_x\bar{S}$ should be increase after Fe_2O_3 incorporated in $C_4A_{3-x}F_x\bar{S}$, but the variations of the unit cell are inconsistent in different researches. The unit cell of different FR-CSA clinkers are obtained by the Rietveld refinement. As shown in Table 3, the reference crystal structures are $C_4A_3\bar{S}$-o and $C_4A_3\bar{S}$-c. After Rietveld refinement, the unit cells of $C_4A_{3-x}F_x\bar{S}$ in different FR-CSA clinkers are shown in Table 4. With the increase of CaO content in raw material, the lattice constants of cubic cell $C_4A_{3-x}F_x\bar{S}$ decrease gradually. For the orthorhombic cell $C_4A_{3-x}F_x\bar{S}$, the variation of cell parameters *a* and *b* are irregular, but the parameter *c* decreases gradually. These phenomena show a good correlation with other reported results [10, 15, 23].

Table 4 Refined unit cell for $C_4A_{3-x}F_x\bar{S}$

	$C_4A_{3-x}F_x\bar{S}$-c			$C_4A_{3-x}F_x\bar{S}$-o		
	a	b	c	a	b	c
$C_{0.90}$	9.210	9.210	9.210	12.957	13.001	9.220
$C_{0.95}$	9.209	9.209	9.209	12.960	13.000	9.207
$C_{1.00}$	9.207	9.207	9.207	13.087	13.036	9.170
$C_{1.05}$	9.207	9.207	9.207	13.071	13.030	9.168
$C_{1,10}$	9.204	9.204	9.204	13.068	13.029	9.162

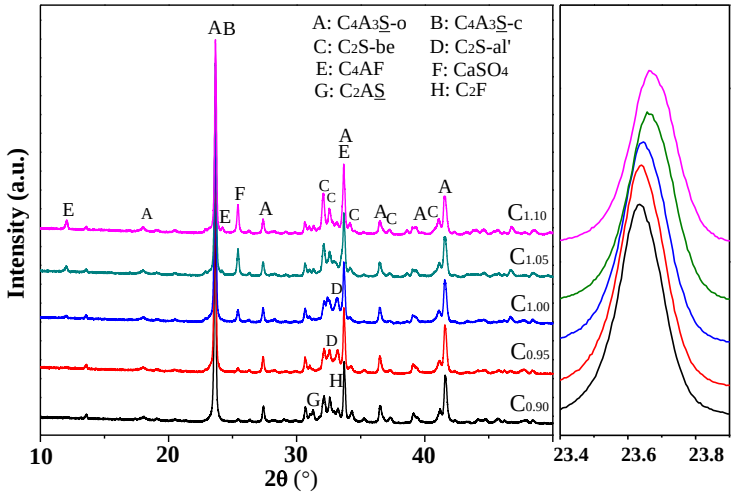

Fig. 1 XRD patterns of the FR-CSA clinkers with different value of C_m in raw materials

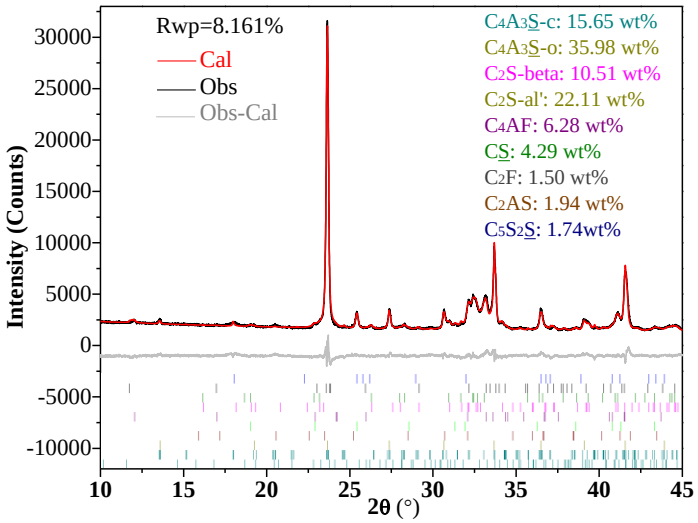

Fig. 2 Rietveld refinement plots of clinker $C_{1.00}$. The black line indicates the experimental scan, the red line indicates the calculation pattern, the middle gray line represents the difference curve, and the short line at the bottom indicates the peak positions of different phases

The mineral compositions of the clinkers were analyzed via RQPA using HighScore Plus software [24, 25]. Fig. 2 shows the Rietveld refinement plots of clinker $C_{1.00}$. The weighted profile R-factor (R_{wp}) is 8.161%. $C_4A_3\bar{S}$ exists in the orthorhombic and cubic crystal structure in the clinker. C_2S exists in the form of beta-C_2S and alpha'-C_2S. The amounts of $CaSO_4$, C_4AF, and C_2F in clinker $C_{1.00}$ are also calculated, as shown in Table 5. Furthermore, the amounts of different phases in clinkers $C_{0.90}$, $C_{0.95}$, $C_{1.05}$, and $C_{1.10}$ are also calculated according to the RQPA results and presented in Table 5. Theoretically, the targeted phases of clinkers include $C_4A_3\bar{S}$, C_2S, C_4AF, and $CaSO_4$. However, the phase formation is complicate and uncontrollable in the CaO–Al_2O_3–Fe_2O_3–SO_3–SiO_2 system [26]. Thus, small amounts of C_2F, $C_5S_2\bar{S}$, and C_2AS are also formed in the FR-CSA clinkers, resulting in the difference between the theoretical and quantified phases. With the increase of the amount of CaO in raw material, the contents of $C_4A_3\bar{S}$ and C_2AS decrease, while the amount of C_4AF, $CaSO_4$, and C_2F increases.

For the clinker $C_{0.90}$, the amount of CaO is too small to exhaust Al_2O_3, Fe_2O_3, and SiO_2 during the calcination process. When CaO in the forms of $Ca(OH)_2$ and $CaCO_3$ are completely consumed, additional CaO from decomposing of $CaSO_4$ is required to continue to react with Al_2O_3, Fe_2O_3 or SiO_2, which promotes the decomposition of $CaSO_4$. However, for the clinker $C_{1.10}$, the amount of CaO is enough to react with Al_2O_3, Fe_2O_3, and SiO_2 according to the stoichiometric raw mixture, with only minor decomposition of $CaSO_4$. Thus, the amount of $CaSO_4$ in FR-CSA clinker increases with increasing in CaO. In addition, although the values of C_m are higher than 1.00 for clinkers $C_{1.05}$ and $C_{1.10}$, but f-CaO does not exist in all the clinkers. Therefore, the properties of FR-CSA cement will not be influenced by f-CaO.

Table 5 Phase compositions of different clinkers (wt.%) (Theo.: theoretical phases calculated using the Bogue equations. Quant.: phases quantified via Rietveld refinement)

Clinkers / Mineral	Theo.	Quant.				
		$C_{0.90}$	$C_{0.95}$	$C_{1.00}$	$C_{1.05}$	$C_{1.10}$
$C_4A_3\bar{S}$-o	—	14.89	16.21	15.65	16	15.23
$C_4A_3\bar{S}$-c	—	40.65	37.94	35.98	31.28	28.15

$C_4A_3\bar{S}$	**40**	**55.84**	**54.15**	**51.63**	**46.98**	**43.38**
C_2S-beta	—	25.04	17.2	10.51	11.47	27.77
C_2S-alpha'	—	8.71	15.75	22.11	20.17	4.5
C_2S	**30**	**33.75**	**32.95**	**32.62**	**31.64**	**32.27**
$CaSO_4$	**10**	**0.54**	**1.91**	**4.29**	**7.76**	**8.47**
C_2AS	—	5.09	2.79	1.94	1.41	0.95
$C_5S_2\bar{S}$	—	1.16	1.79	1.74	2.41	2.99
C_4AF	**20**	**2.60**	**4.93**	**6.28**	**7.92**	**9.35**
C_2F	—	1.02	1.48	1.5	1.88	2.59

3.1.2 Incorporation levels of Fe_2O_3 in $C_4A_{3-x}F_x\bar{S}$

The experimentally quantified $C_4A_3\bar{S}$ content, theoretical calculated $C_4A_3\bar{S}$ content, and the differences between them are shown in Fig. 3. The theoretical content of $C_4A_3\bar{S}$ in different clinkers are 40 wt.%, but the experimental results are different. With increasing amount of CaO in the raw materials, the amount determined by experiments and its deviation from theoretical amounts of $C_4A_3\bar{S}$ phase decrease significantly. Since the cell parameters of $C_4A_3\bar{S}$ and $C_4A_{3-x}F_x\bar{S}$ phases are similar, the $C_4A_3\bar{S}$ content determined by experiments actually consists of the $C_4A_{3-x}F_x\bar{S}$ and pure $C_4A_3\bar{S}$. When some amount of Fe_2O_3 are incorporated in $C_4A_3\bar{S}$ to form $C_4A_{3-x}F_x\bar{S}$, different incorporation levels lead to the variation of the amount of $C_4A_3\bar{S}$ phase determined by experiments. For the Fe_2O_3 in the FR-CSA clinker, in addition to forming C_4AF and C_2F, the remaining Fe_2O_3 replace Al_2O_3 in $C_4A_{3-x}F_x\bar{S}$. Hence, according to previous research[27], the amount of Fe_2O_3 involved in the substitution reaction is calculated using the Fe_2O_3 content in C_4AF and C_2F. The substitution amount of Fe_2O_3 and the values of x in $C_4A_{3-x}F_x\bar{S}$ are calculated and presented in Table 6. With increasing CaO content in raw material, the incorporation levels of Fe_2O_3 in $C_4A_{3-x}F_x\bar{S}$ decrease from 17.41 wt.% to 8.89 wt.%. The values of x in $C_4A_{3-x}F_x\bar{S}$ decrease from 0.36 to 0.18 correspondingly.

Table 6 Substitution amount of Fe_2O_3 in $C_4A_{3-x}F_x\bar{S}$

Clinkers	Substitution amount (wt.%)	X
$C_{0.90}$	17.72	0.36
$C_{0.95}$	14.66	0.30
$C_{1.00}$	13.69	0.28
$C_{1.05}$	11.92	0.24
$C_{1.10}$	8.96	0.18

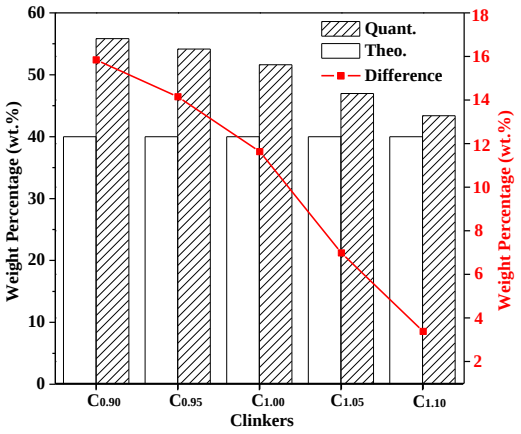

Fig. 3 Quantitative and theoretical amount of $C_4A_3\bar{S}$ and the differences between them for different FR-CSA clinkers

3.1.3 Analysis of mineral compositions by FT-IR

To verify the variation of the mineral composition among the FR-CSA clinkers, FT-IR was used to measure the chemical bonds of different phases in the FR-CSA clinkers. Infrared absorption spectra of $C_{0.90}$, $C_{0.95}$, $C_{1.00}$, $C_{1.05}$, and $C_{1.10}$ are shown in Fig. 4. The vibration frequencies of the clinkers are in the range of 400–1400 cm^{-1}. As shown in Fig. 4, the absorption bands corresponding to $C_4A_{3-x}F_x\bar{S}$, $CaSO_4$, and C_2S are intense, while the bands of C_2AS, $C_5S_2\bar{S}$, and C_2F are hardly observed due to their low content in all the clinkers. The appearance and increase in the intensities of the IR bands located at about 595 cm^{-1} result from the vibrations of Fe–O bonds in $[FeO_4]$ tetrahedral structural units[28]. The bending vibration of the $[SO_4]$ tetrahedron in $CaSO_4$ is identified at 617 cm^{-1} and the stretching vibration of S-O for the $[SO_4]$ groups is observed at 1156 and 1195 cm^{-1}. The enhancement of these bands is observed in the clinkers with a C_m ranging from 0.90 to 1.10, which is consistent with the results from XRD analysis. The groups of $[SO_4]$ in $C_4A_{3-x}F_x\bar{S}$ are identified at 619, 663, and 987 cm^{-1}, which are almost identical to the wavenumbers of the bands corresponding to $[SO_4]$ groups in the $CaSO_4$[29, 30]. However, the bands observed at 1100 cm^{-1} exhibit a shift to a higher wavenumber with the addition of CaO in raw materials. This is because there are differences in the coordination environment of the $[SO_4]$ group due to the incorporation of Fe_2O_3 in $C_4A_{3-x}F_x\bar{S}$. The absorption bands located at 411, 644, 690, 821, and 875 cm^{-1} are assigned to $[AlO_4]$ groups in the $C_4A_{3-x}F_x\bar{S}$ mineral[15, 31]. With the increase of the CaO content in raw material, the band observed at 821 cm^{-1} shifted to smaller wavenumber due to the decrease of Fe/Al in the $C_4A_{3-x}F_x\bar{S}$ mineral. All of these phenomena are consistent with the results concluded by XRD analysis.

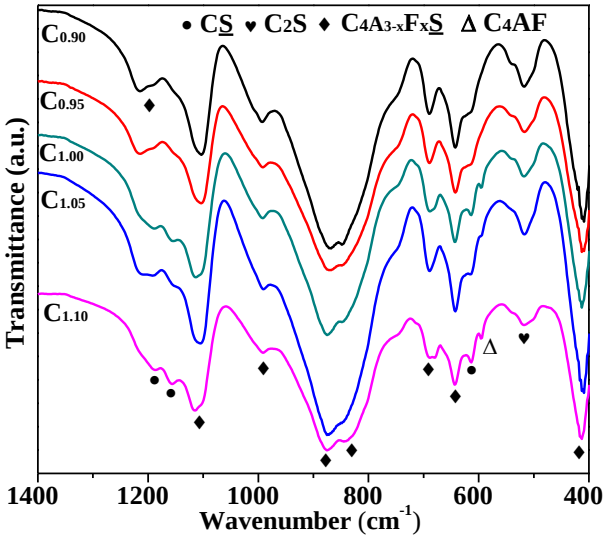

Fig. 4 FT-IR of clinkers $C_{0.90}$–$C_{1.10}$

3.1.4 Distribution of Fe_2O_3 in iron-bearing minerals of the FR-CSA clinker

The SEM images of clinkers with a C_m ranging from 0.90 to 1.10 are presented in Fig. 5. The $C_4A_{3-x}F_x\bar{S}$ exhibits a hexagonal platy structure or a quadrilateral columnar structure on the micro-level. As shown in Fig. 5, with increasing CaO content in raw material, the amount of hexagonal platy grains decreased slightly, which is consistent with the amount of $C_4A_{3-x}F_x\bar{S}$ from XRD analysis.

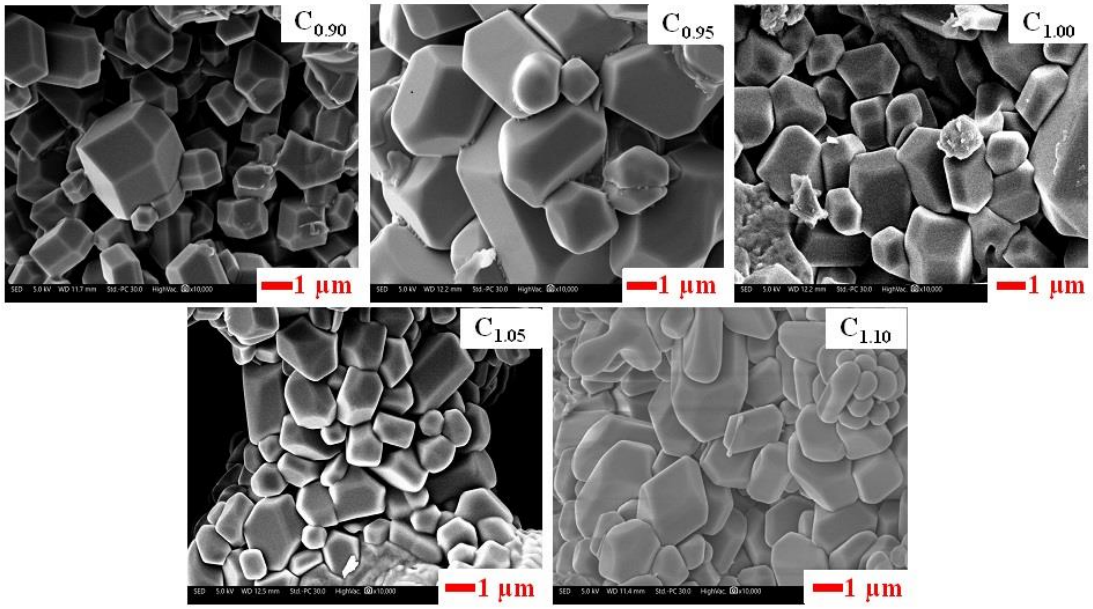

Fig. 5 SEM images of clinkers $C_{0.90}$-$C_{1.10}$

To verify the proportion of Fe_2O_3 in the $C_4A_{3-x}F_x\bar{S}$, the elemental compositions of the $C_4A_{3-x}F_x\bar{S}$ grains are detected via SEM/EDS analysis. Five different $C_4A_{3-x}F_x\bar{S}$ grains in clinker $C_{1.00}$ are selected to detect the elemental composition. The results are summarized in Fig. 6 and Table 7. The main elements (i.e., O, Ca, Al, Fe, and S) are presented in the mapping picture, and their mass fraction are listed in Table 7. The mass ratio of S: Ca: O is about 1: 5: 8, which is the chemical composition of $C_4A_3\bar{S}$. Furthermore, the total content of Fe_2O_3 mixed with Al_2O_3 are various in different grains, but the average Fe_2O_3 content in $C_4A_{3-x}F_x\bar{S}$ grains is approximately 14.08 wt.% for clinker $C_{1.00}$. It is consistent with the result calculated via quantitative XRD analysis.

Similarity, another four clinkers are also tested via SEM/EDS according to this method. The results are also presented in Table 7. The incorporation levels of Fe_2O_3 in $C_4A_{3-x}F_x\bar{S}$ decrease with increasing CaO content in raw material. Furthermore, the incorporation levels of Fe_2O_3 in $C_4A_{3-x}F_x\bar{S}$ calculated by two methods are consistent. The results further demonstrate that the content of Fe_2O_3 incorporated in $C_4A_{3-x}F_x\bar{S}$ decreased with increasing CaO content in raw materials.

Table 7 Chemical composition of areas in the $C_4A_{3-x}F_x\bar{S}$ grains (wt.%)

Clinkers	Areas	O	Ca	Al	Fe	S	$W(Fe_2O_3)/ W(Al_2O_3+ Fe_2O_3)$
	1	41.73	24.03	22.38	4.47	5.23	13.12
	2	42.08	24.83	19.93	5.29	5.46	16.71
$C_{1.00}$	3	42.34	24.14	21.86	4.14	5.27	12.52
	4	41.94	22.66	22.31	5.04	5.92	14.59
	5	42.49	24.68	21.63	4.43	5.18	13.41
$C_{0.90}$	Average	42.21	24.30	20.40	5.55	5.32	17.06
$C_{0.95}$	Average	42.39	24.16	20.96	4.64	5.69	14.34
$C_{1.00}$	Average	42.11	24.06	21.62	4.67	5.42	14.04
$C_{1.05}$	Average	43.44	23.88	21.94	3.88	5.53	11.79
$C_{1.10}$	Average	43.66	22.95	22.14	3.14	6.18	9.68

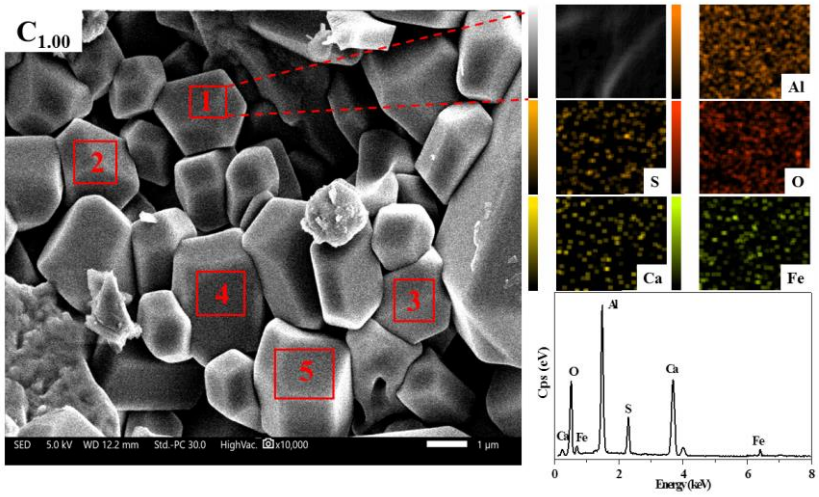

Fig. 6 SEM/EDS image and elemental composition map of clinker $C_{1.00}$

3.1.5 Effective utilization rate of Fe_2O_3 and Al_2O_3

As shown in Fig. 7, the ratios of Fe_2O_3 and Al_2O_3 distributed in different phases are presented respectively. With the increase of CaO content in raw material, fewer Fe_2O_3 participate in the formation of $C_4A_{3-x}F_x\bar{S}$. Compared with the clinker $C_{0.90}$, about 50 wt.% Fe_2O_3 transfer into C_4AF and C_2F from $C_4A_{3-x}F_x\bar{S}$ in clinker $C_{1.10}$. Because the hydration activity of $C_4A_{3-x}F_x\bar{S}$ is more beneficial to the performance of the CSA cement based binders than that of C_4AF and C_2F[23], increasing CaO is not conducive to the effective utilization of Fe_2O_3. For the distribution of Al_2O_3, although the amount of $C_4A_{3-x}F_x\bar{S}$ decreases obviously, the ratios of Al_2O_3 distributed in them are almost unchanged, and all of them can reach to 90 wt.%. With the increasing CaO content in raw material, the Al_2O_3 content in the form of C_2AS decreases, while Al_2O_3 content in the form of C_4AF increases. It is beneficial to the mechanical property development of FR-CSA cement because C_4AF has higher hydration reactivity than C_2AS. Therefore, increasing the amount of CaO in raw material can improve the effective utilization of Al_2O_3, but it inhibits Fe_2O_3 incorporation in $C_4A_{3-x}F_x\bar{S}$.

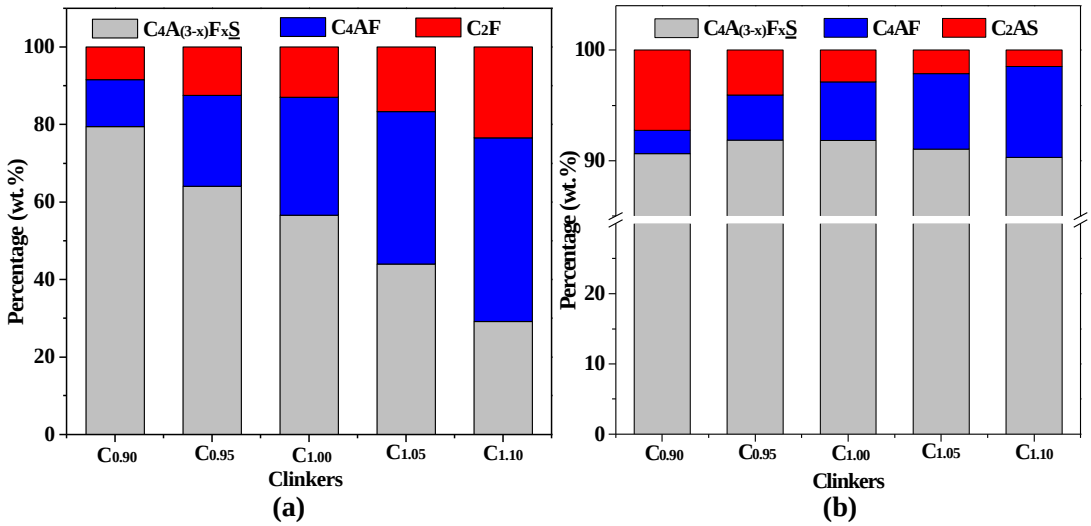

Fig. 7 Ratios of Fe_2O_3 and Al_2O_3 distributed in different minerals (a: Fe_2O_3, b: Al_2O_3)

3.2 Effect of CaO content on iron-bearing phase composition of FR-CSA clinker with 30 wt.% C_4AF

The effect of CaO on the phase composition of FR-CSA clinker is investigated based on FR-CSA clinker with 30 wt.% C_4AF. The XRD patterns of these clinkers are shown in Fig. 8. The types of

minerals in clinkers are almost the same with those in the FR-CSA clinker with 20 wt.% C_4AF. For the FR-CSA clinker with 30 wt.% C_4AF and a C_m of 0.90, the XRD peaks of $CaSO_4$ are detected. The characteristic peaks of C_2AS don't exist in the FR-CSA clinker. More importantly, with increasing CaO content in raw materials, the C_4AF content increases clearly and the main characteristic peak of $C_4A_{3-x}F_x\bar{S}$ also shifts to higher angles. It conclude that the incorporation content of Fe_2O_3 in $C_4A_{3-x}F_x\bar{S}$ also decrease with increasing of CaO content in raw material, which is consistent with the phenomenon that 20 wt.% C_4AF is designed in the FR-CSA clinker.

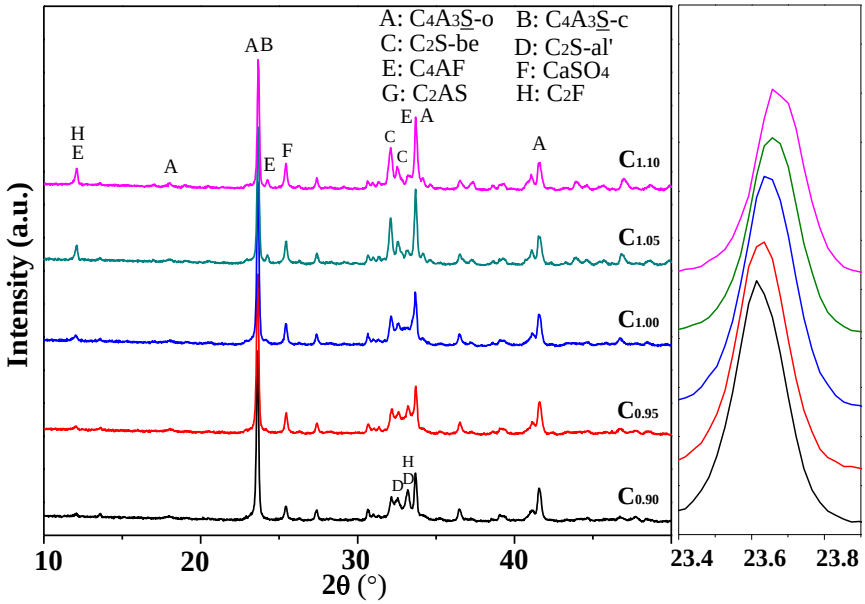

Fig. 8 XRD patterns of the FR-CSA clinkers with 30 wt.% C_4AF content designed

Thus, during the calcination process of FR-CSA clinker, the CaO content in raw material influence the phase composition of clinker. With the increase of CaO content, the incorporation level of Fe_2O_3 in $C_4A_{3-x}F_x\bar{S}$ decreases, which led to more C_4AF and fewer $C_4A_{3-x}F_x\bar{S}$ formed.

3.3 Effect of CaO in the form of $CaSO_4$ on iron-bearing phase formation of FR-CSA clinker

Fig. 9 presents the XRD patterns of FR-CSA clinkers designed with different extra amounts of $CaSO_4$, respectively. It demonstrates that a part of CaO in the form of $CaSO_4$ doesn't react with other materials during the calcination process. In the proportion design of the raw mixture, all of CaO in the form of $CaSO_4$ are used to calculate the value of C_m. However, $CaSO_4$ doesn't fully decompose for the clinkers with the extra amount of $CaSO_4$ more than 5 wt.%. Thus the C_m values are actually less than 1.00. Moreover, when the extra amount of $CaSO_4$ of clinkers increases from 0 to 20 wt.%, the amount of undecomposed $CaSO_4$ also increases. That is to say, the amount of CaO involved in the calcination reaction decreases, which restricts the reaction of C_2AS consumption according to Eq. 5, the amount of C_2AS increases in FR-CSA clinkers.

In addition, with increasing exctra $CaSO_4$ content in raw materials, the C_4AF content in clinkers decreases, while the differences between the theoretically calculated and experimentally determined content of $C_4A_{3-x}F_x\bar{S}$ increase. Meanwhile, the highest peak of $C_4A_{3-x}F_x\bar{S}$ also shifts to lower angles according to their XRD patterns and the d-spaces of them increase from 3.7520 to 3.7614 Å. It demonstrates that the volume of the unit cell structure of $C_4A_{3-x}F_x\bar{S}$ increases. Thus, according to the change of unit cell structure and the variation of mineral composition, it is concluded that the content of Fe_2O_3 incorporated in $C_4A_{3-x}F_x\bar{S}$ increases with increasing extra $CaSO_4$ content in raw material

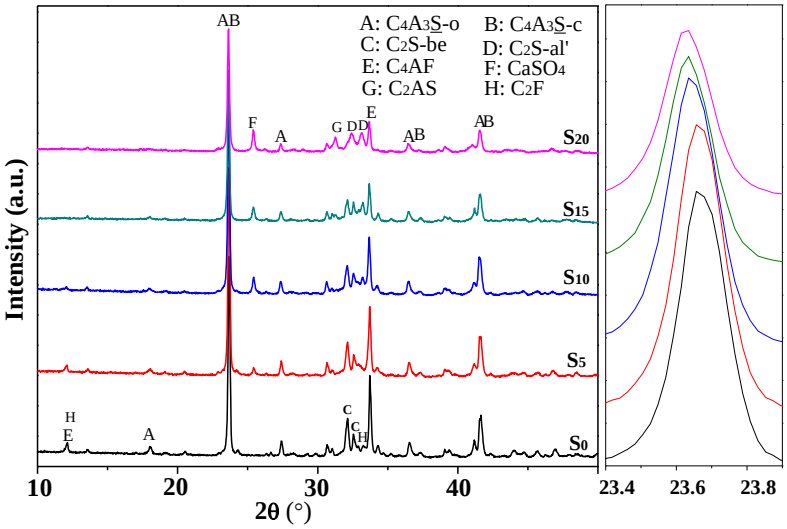

Fig. 9 XRD patterns of the FR-CSA clinkers with different $CaSO_4$ content in raw materials

In a word, with increasing extra $CaSO_4$ content in raw materials, the CaO content involved in chemical reaction during calcination process decreases, leading to the increase of Fe_2O_3 content incorporated in $C_4A_{3-x}F_x\bar{S}$. It is consistent with the variation caused by changes in CaO content.

3.4 Effect of CaO content variation caused by calcination temperature and holding time on the iron-bearing phase formation of FR-CSA clinker

Calcination temperature and holding time during calcination process of the FR-CSA clinker not only affect the formation of reactive minerals but also can affect the decomposition of $CaSO_4$. Thus the effects of calcination temperature and holding time on the iron-bearing phase composition of the FR-CSA clinker were also investigated. The XRD results are shown in Fig. 10.

With the increase of calcination temperature, the intensity of $CaSO_4$ diffraction peaks decrease and disappear finally. It means that more $CaSO_4$ were decomposed, resulting in that more CaO participate in the mineral formation during the calcination process. Meanwhile, the intensity of C_4AF diffraction peaks increases, while the intensity of $C_4A_{3-x}F_x\bar{S}$ decreases. It demonstrates that the content of Fe_2O_3 incorporated in the $C_4A_{3-x}F_x\bar{S}$ decreases with the increase in calcination temperature. Similarly, as shown in Fig. 10(b), with the increase in holding time, the intensity of $CaSO_4$ diffraction peaks decrease and those of C_4AF increase. It is consistent with the phenomenon caused by the changing of calcination temperature. Increasing the calcination temperature and holding time cause more CaO to participate in the mineral formation reaction, accompanied by an increase in C_4AF content and a decrease in $C_4A_{3-x}F_x\bar{S}$ content, which further demonstrates that more CaO content involved in the reaction can make less Fe_2O_3 incorporated in $C_4A_{3-x}F_x\bar{S}$. Therefore, when the calcination temperature is between 1200 ℃ to 1300 ℃, the effects of calcination temperature and holding time on the iron-bearing phase composition are mainly caused by their influence on the decomposition degree of $CaSO_4$ and the content of CaO involved in mineral formation reactions.

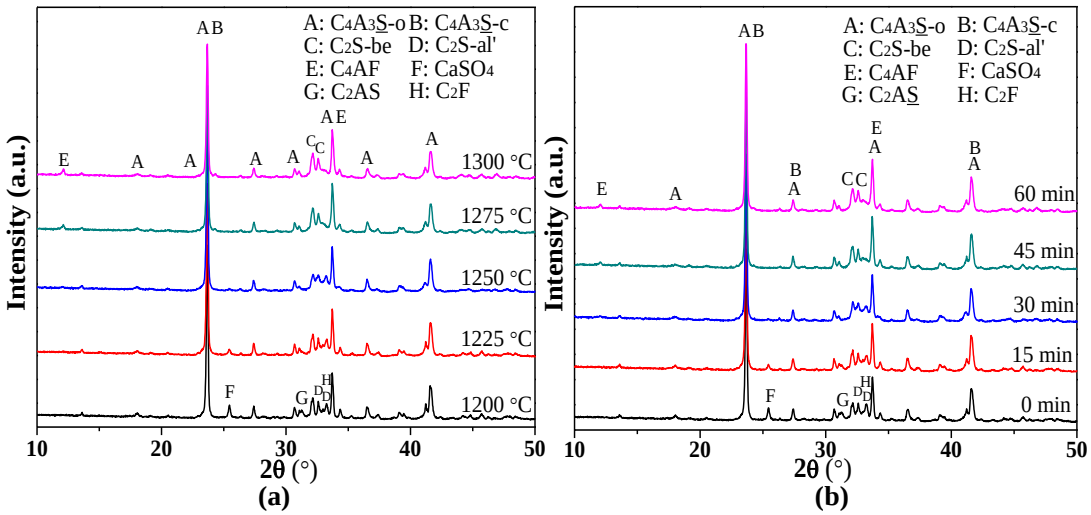

Fig. 10 XRD patterns of the FR-CSA clinkers with different calcination temperature and maintained time (a: Different temperature, b: Different holding time)

4. Conclusion

This research demonstrated the effect of CaO content in raw material on iron-bearing phase composition of FR-CSA clinker. The CaO content in raw material significantly influences the phase formation in the FR-CSA clinker during the calcination process, especially for the formation of iron-bearing phases.

With the reduction of CaO content in the form of $CaCO_3$ or $Ca(OH)_2$ in raw materials, the amount of C_4AF formed in the FR-CSA clinkers decreased and the amount of Fe_2O_3 incorporated in $C_4A_{3-x}F_x\bar{S}$ increased. When the C_m is 0.90 and 20 wt.% C_4AF are designed in the FR-CSA clinker, the value of x in the $C_4A_{3-x}F_x\bar{S}$ can be up to 0.36.

For the CaO content existed in the form of $CaSO_4$ in raw material, it presents a similar effect. When the CaO content is constant and the $CaSO_4$ content increases in raw material, the CaO content involved in the calcination reaction decreased, which also lead to an increase in the amount of Fe_2O_3 incorporated in $C_4A_{3-x}F_x\bar{S}$.

The findings in this study make it possible to optimize the mineral composition of the FR-CSA clinker by changing the CaO content in the raw materials. Furthermore, low CaO content in raw material is beneficial to the formation of $C_4A_{3-x}F_x\bar{S}$, which enables that some solid wastes containing low calcium or low aluminum can also be used as raw materials for FR-CSA cement production.

Acknowledgments

The authors acknowledge the support of the National Key Research & Development Program of China (No. 2017YFC0703100), Shandong Provincial Major Scientific and Technological Innovation Project (No. 2019JZZY020306). This research is also funded by the China Scholarship Council.

References

[1] Zhang L, Su MZ, Wang YM. Development of the use of sulfo- and ferroaluminate cements in China. Advances In Cement Research. 1999;11(1):15-21.

[2] Glasser FP, Zhang L. High-performance cement matrices based on calcium sulfoaluminate-belite compositions. Cement And Concrete Research. 2001;31(12):1881-6.

[3] Chen M, Liu B, Li L, Cao L, Huang Y, Wang S, et al. Rheological parameters, thixotropy and creep of 3D-printed calcium sulfoaluminate cement composites modified by bentonite. Composites Part B: Engineering. 2020:107821.

[4] Chen IA, Juenger MCG. Synthesis and hydration of calcium sulfoaluminate-belite cements with varied phase compositions. Journal of Materials Science. 2010;46(8):2568-77.

[5] Liu C, Luo J, Li Q, Gao S, Su D, Zhang J, et al. Calcination of green high-belite sulphoaluminate cement (GHSC) and performance optimizations of GHSC-based foamed concrete. Materials & Design. 2019;182:107986.

[6] Hanein T, Galvez-Martos J-L, Bannerman MN. Carbon footprint of calcium sulfoaluminate clinker production. Journal of Cleaner Production. 2018;172:2278-87.

[7] Hargis CW, Kirchheim AP, Monteiro PJM, Gartner EM. Early age hydration of calcium sulfoaluminate (synthetic ye'elimite,) in the presence of gypsum and varying amounts of calcium hydroxide. Cement and Concrete Research. 2013;48:105-15.

[8] Morin V, Termkhajornkit P, Huet B, Pham G. Impact of quantity of anhydrite, water to binder ratio, fineness on kinetics and phase assemblage of belite-ye'elimite-ferrite cement. Cement and Concrete Research. 2017;99:8-17.

[9] Wang YM, Su M, Zhang L. Sulphoaluminate Cement: Press Beijing Univ.

[10] Chen D, Feng XJ, Long SZ. The influence of ferric oxide on the properties of 3CaO·3Al2O3·CaSO4. Thermochimica Acta. 1993;215:157-69.

[11] Möschner G, Lothenbach B, Winnefeld F, Ulrich A, Figi R, Kretzschmar R. Solid solution between Al-ettringite and Fe-ettringite (Ca6[Al1−xFex(OH)6]2(SO4)3·26H2O). Cement and Concrete Research. 2009;39(6):482-9.

[12] Ectors D, Neubauer J, Goetz-Neunhoeffer F. The hydration of synthetic brownmillerite in presence of low Ca-sulfate content and calcite monitored by quantitative in-situ-XRD and heat flow calorimetry. Cement and Concrete Research. 2013;54:61-8.

[13] Cuesta A, Santacruz I, Sanfélix SG, Fauth F, Aranda MAG, De la Torre AG. Hydration of C4AF in the presence of other phases: A synchrotron X-ray powder diffraction study. Construction and Building Materials. 2015;101:818-27.

[14] Huang Y, Shen XD, Ma SH, Chen L, Q. ZB. Effect of Fe2O3 on the formation of calcium sulphoaluminate mineral. Journal of the Chinese Ceramic Society. 2005;35(4):485-9.

[15] Idrissi M, Diouri A, Damidot D, Greneche JM, Talbi MA, Taibi M. Characterisation of iron inclusion during the formation of calcium sulfoaluminate phase. Cement and Concrete Research. 2010;40(8):1314-9.

[16] Touzo B, Scrivener KL, Glasser FP. Phase compositions and equilibria in the CaO–Al2O3–Fe2O3–SO3 system, for assemblages containing ye'elimite and ferrite Ca2(Al,Fe)O5. Cement and Concrete Research. 2013;54:77-86.

[17] Berrio A, Rodriguez C, Tobón JI. Effect of Al2O3/SiO2 ratio on ye'elimite production on CSA cement. Construction and Building Materials. 2018;168:512-21.

[18] Ren C, Wang W, Li G. Preparation of high-performance cementitious materials from industrial solid waste. Construction and Building Materials. 2017;152:39-47.

[19] Shen Y, Qian J, Huang Y, Yang D. Synthesis of belite sulfoaluminate-ternesite cements with phosphogypsum. Cement and Concrete Composites. 2015;63:67-75.

[20] Yao X, Wang W, Liu M, Yao Y, Wu S. Synergistic use of industrial solid waste mixtures to prepare ready-to-use lightweight porous concrete. Journal of Cleaner Production. 2019;211:1034-43.

[21] Wu S, Wang W, Ren C, Yao X, Yao Y, Zhang Q, et al. Calcination of calcium sulphoaluminate cement using flue gas desulfurization gypsum as whole calcium oxide source. Construction and Building Materials. 2019;228:116676.

[22] O. Andac FPG. Polymorphism of calcium sulphoaluminate (Ca4A160 16 • S03) and its solid solutions. Advances in Cement Research. 1994;22(6):57-60.

[23] Bullerjahn F, Schmitt D, Ben Haha M. Effect of raw mix design and of clinkering process on the formation and mineralogical composition of (ternesite) belite calcium sulphoaluminate ferrite clinker. Cement and Concrete Research. 2014;59:87-95.

[24] Álvarez-Pinazo G, Cuesta A, García-Maté M, Santacruz I, Losilla ER, la Torre AGD, et al. Rietveld quantitative phase analysis of Yeelimite-containing cements. Cement and Concrete Research. 2012;42(7):960-71.

[25] Cuberos AJ, De la Torre AG, Alvarez-Pinazo G, Martin-Sedeno MC, Schollbach K, Pollmann H, et al. Active iron-rich belite sulfoaluminate cements: clinkering and hydration. Environmental science & technology. 2010;44(17):6855-62.

[26] Sahu S, Majling J. Phase compatibility in the system CaO-SiO2-Al2O3-Fe2O3-SO3 referred to sulphoaluminate belite cement clinker. Cement and Concrete Research. 1993;23(6):1331-9.

[27] Yao X, Yang S, Huang Y, Wu S, Yao Y, Wang W. Effect of CaSO4 batching in raw material on the iron-bearing mineral transition of ferric-rich sulfoaluminate cement. Construction and Building Materials. 2020;250:118783.

[28] Rada S, Dehelean A, Culea E. FTIR, Raman, and UV-Vis spectroscopic and DFT investigations of the structure of iron-lead-tellurate glasses. J Mol Model. 2011;17(8):2103-11.

[29] Montes M, Pato E, Carmona-Quiroga PM, Blanco-Varela MT. Can calcium aluminates activate ternesite hydration? Cement and Concrete Research. 2018;103:204-15.

[30] Julphunthong P. Synthesizing of calcium sulfoaluminate-belite (CSAB) cements from industrial waste materials. Materials Today: Proceedings. 2018;5(7):14933-8.

[31] Guo Y, Deng J, Su M, Wang Y. A study on formation mechnism of ferrite phase in ferroaluminate cement. Journal of the Chinese Ceramic Society. 1988;16(6):481-8.